Received: 3 March 2017 | Accepted: 10 April 2017

DOI: 10.1111/jace.14929

ORIGINAL ARTICLE

Journal of the American Ceramic Society

High quality factor microwave dielectric ceramics in the $(Mg_{1/3}Nb_{2/3})O_2$–ZrO_2–TiO_2 ternary system

Wen-Bo Li[1] | Di Zhou[1,2,3] | Li-Xia Pang[3,4] | Yan-Zhu Dai[1] | Ze-Ming Qi[5] | Qiu-Ping Wang[6] | Han-Chen Liu[6]

[1]Electronic Materials Research Laboratory, Key Laboratory of the Ministry of Education & International Center for Dielectric Research, Xi'an Jiaotong University, Xi'an, Shaanxi, China

[2]Xi'an Jiaotong University Suzhou Academy, Suzhou, Jiangsu, China

[3]Department of Materials Science and Engineering, University of Sheffield, Sheffield, UK

[4]Micro-optoelectronic Systems Laboratories, Xi'an Technological University, Xi'an, Shaanxi, China

[5]National Synchrotron Radiation Laboratory, University of Science and Technology of China, Anhui, Hefei, China

[6]School of Science, Xi'an Polytechnic University, Xi'an, China

Correspondence
Di Zhou, Electronic Materials Research Laboratory, Key Laboratory of the Ministry of Education & International Center for Dielectric Research, Xi'an Jiaotong University, Xi'an, Shaanxi, China.
Email: zhoudi1220@gmail.com

Funding information
the National Natural Science Foundation of China, Grant/Award Number: U1632146; the Young Star Project of Science and Technology of Shaanxi Province, Grant/Award Number: 2016KJXX-34, 2015KJXX-39; the Fundamental Research Funds for the Central University, and the 111 Project of China, Grant/Award Number: B14040

Abstract

Novel high quality factor microwave dielectric ceramics $(1-x)ZrTiO_4-x(Mg_{1/3}Nb_{2/3})TiO_4$ $(0.325\leq x\leq 0.4)$ and $(ZrTi)_{1-y}(Mg_{1/3}Nb_{2/3})_yO_4$ $(0.2\leq y\leq 0.5)$ with the addition of 0.5 wt% $MnCO_3$ in the $(Mg_{1/3}Nb_{2/3})O_2$–ZrO_2–TiO_2 ternary system were prepared, using solid-state reaction method. The relationship between the structure and microwave dielectric properties of the ceramics was studied. The XRD patterns of the sintered samples reveal the main phase belonged to α-PbO_2-type structure. Raman spectroscopy and infrared reflectivity (IR) spectra were employed to evaluate phonon modes of ceramics. The $0.65ZrTiO_4-0.35(Mg_{1/3}Nb_{2/3})TiO_4$−0.5 wt% $MnCO_3$ ceramic can be well densified at 1240°C for 2 hours and exhibits good microwave dielectric properties with a relative permittivity (ε_r) of 42.5, a quality factor ($Q\times f$) value of 43 520 GHz (at 5.9 Ghz) and temperature coefficient of resonant frequency (τ_f) value of −5ppm/°C. Furthermore, the $(ZrTi)_{0.7}(Mg_{1/3}Nb_{2/3})_{0.3}O_4$−0.5 wt% $MnCO_3$ ceramic sintered at 1260°C for 2 hours possesses a ε_r of 31.8, a $Q\times f$ value of 35 640 GHz (at 6.3 GHz) and a near zero τ_f value of −5.9 ppm/°C. The results demonstrated that the $(Mg_{1/3}Nb_{2/3})O_2$–ZrO_2–TiO_2 ternary system with excellent properties was a promising material for microwave electronic device applications.

KEYWORDS
dielectric materials/properties, phase diagrams, solid solutions, sinter/sintering

1 | INTRODUCTION

Microwave communication technology has been widely studied and made remarkable progress in the past decades for practical application.[1-5] Microwave dielectric ceramics have been used as components extensively in the filters units of communication systems, such as wireless fidelity (WIFI), global positioning systems (GPS) patch antennas, and mobile telephones, etc.[6-10] In particular, dielectric resonator has a very important position in microwave integrated circuits and microwave filters. Microwave dielectric ceramics with high-dielectric permittivities (ε_r), high quality factor ($Q\times f$), small or zero temperature coefficient of resonant frequency (τ_f) and nontoxic constituents are indispensable for microwave devices.[11,12]

The binary system ZrO_2–TiO_2 has been studied as good candidates for microwave dielectric materials in the last two decades. Previous studies show that $ZrTiO_4$ based solid solutions with α-PbO_2 type structure have been widely used as dielectric resonators because of good microwave dielectric properties.[13-15] The studies conduct that Zr^{4+} ions or Ti^{4+} ions substitution by M^{4+} ions has a significant impact on the microwave dielectric properties of ZrO_2–TiO_2 system. It was found that the $Zr_xSn_yTi_zO_4$ ($x+y+z=2$) system has superior microwave dielectric properties, near zero τ_f value and high $Q\times f$ value.[16] Due to the difference between the ionic radii of Zr^{4+} ions (0.72 Å, CN=6) and Ti^{4+} ions (0.53 Å, CN=6), ZrO_2–TiO_2 binary system substitution by $(AB)^{4+}$ ions have been investigated.[17] Such as $Zn_{1/3}Ta_{2/3}O_2$–ZrO_2–TiO_2 ternary system, $Zn_{1/3}Nb_{2/3}O_2$–ZrO_2–TiO_2 ternary system and $Zr(Zn_{1/3}Nb_{2/3})_xTi_{2-x}O_6$.[18-22] It is well known that the microwave dielectric ceramic $Zn_{1/3}Ta_{2/3}O_2$–ZrO_2–TiO_2 ternary system has been investigated extensively. For example, Kim et al. showed that $Zr_{1-x}(Zn_{1/3}Ta_{2/3})_xTiO_4$ ($0.2\le x\le 0.6$) with increasing $Zn_{1/3}Ta_{2/3}O_2$ content, two-phase regions were observed: α-PbO_2 solid solution region below $x<0.35$, rutile type $Zn_{1/3}Ta_{2/3}TiO_4$, and the α-PbO_2 solid solution with further substitution of $Zn_{1/3}Ta_{2/3}O_2$. $Zr_{0.65}(Zn_{1/3}Ta_{2/3})_{0.35}TiO_4$ ceramic has good microwave dielectric properties with ε_r=42.5, $Q\times f$=40 200 GHz and τ_f=1.1 ppm/°C.[23] As is known to all, the expensive price and high toxicity of Ta-based materials maybe limited by the $Zn_{1/3}Ta_{2/3}O_2$–ZrO_2–TiO_2 ternary system in practical applications. A series of other $(AB)^{4+}$ ions such as $(Zn_{1/3}Nb_{2/3})^{4+}$ and $(Li_{1/4}Nb_{3/4})^{4+}$ have been attracted by researcher attention. Recently Huang et al. reported that Nb^{5+} (0.64 Å, CN=6) ion replacing Ta^{5+} (0.64 Å, CN=6) ion form the $Zr_x(Zn_{1/3}Nb_{2/3})_{1-x}TiO_4$ (x=0.1-0.4) solid solutions with high ε_r=51, $Q\times f$=26 600 GHz and τ_f=70 ppm/°C.[24] Our previous work investigated $(Li_{1/4}Nb_{3/4})^{4+}$-doped ZrO_2–TiO_2 system and found that crystalline phases and microwave dielectric properties of $(Li_{1/4}Nb_{3/4})_{0.4}Zr_xTi_yO_4$ depended greatly on the Zr/Ti ratio.[25,26] In our work, pure $(Mg_{1/3}Nb_{2/3})TiO_4$ ceramic can be well densified at 1220°C for 2 hours and exhibits good microwave dielectric properties with a ε_r of 81.9, a $Q\times f$ value of 13 380 GHz (at 4.5 GHz) and τ_f value of +277.5 ppm/°C.

In the present work, we investigated the structure and microwave dielectric properties of the $Mg_{1/3}Nb_{2/3}O_2$–ZrO_2–TiO_2 ternary system. Figure 1 presents phase diagram of the $Mg_{1/3}Nb_{2/3}O_2$–ZrO_2–TiO_2 ternary system. As seen from Figure 1, the $ZrTiO_4$–$(Mg_{1/3}Nb_{2/3})TiO_4$ and $(ZrTi)_{1-y}(Mg_{1/3}Nb_{2/3})_yO_4$ phases regions were highlighted by the green line and the red line, respectively. In this system, novel solid solution 0.5 wt% $MnCO_3$-doped $(1-x)ZrTiO_4-x(Mg_{1/3}Nb_{2/3})TiO_4$ ($0.325\le x\le 0.4$) and $(ZrTi)_{1-y}(Mg_{1/3}Nb_{2/3})_yO_4$ ($0.2\le y\le 0.5$) ceramics were prepared, using solid-state reaction method. Sintering behavior, phase composition, microstructures, microwave dielectric properties, and the relation between structure and microwave dielectric properties of the ceramics were studied in detail.

2 | EXPERIMENTAL PROCEDURE

The starting materials of ZrO_2 (≥99%), MgO (>98%), Nb_2O_5 (>99%), TiO_2 (>99.84%), and $MnCO_3$ (>98%) were used according to the stoichiometric formula $(1-x)ZrTiO_4-x(Mg_{1/3}Nb_{2/3})TiO_4$ ($0.325\le x\le 0.4$) and $(ZrTi)_{1-y}(Mg_{1/3}Nb_{2/3})_yO_4$ ($0.2\le y\le 0.5$) with 0.5 wt% $MnCO_3$. Powders were mixed with the Zirconia balls in ethanol and milled for 4 hours, using a planetary mill operating at a running speed of 150 rpm. After being milled, two kinds of powders were calcined at 1000°C and 1100°C for 4 hours, respectively. After being crushed, the powders were remilled for 5 hours to increase reactivity and homogeneity and then dried. The as-dried powders were mixed with 5 wt% polyvinyl alcohol (PVA) binder and granulated, and then these powders were pressed into cylinders (10 mm in diameter and 4~5 mm in height) in a steel die under a uniaxial pressure of 200 MPa. Samples were sintered in the temperature ranges from 1200°C to 1260°C for 2 hours in ambient atmosphere, respectively.

The crystalline structures of samples were investigated, using X-ray diffraction (XRD) with Cu$K\alpha$ radiation (Rigaku D/MAX-2400 X-ray diffractometer, Tokyo, Japan, λ=1.54056 Å) at a scanning rate of $0.02°s^{-1}$ in a 2θ range of 10°-70°. Microstructures of the sintered ceramic were characterized with scanning electron microscopy (SEM) (SEM; Quanta 250 F, FEI). The Raman spectra were recorded at room temperature, using a Raman spectrometer (inVia, Renishaw, England) excited with an Ar^+ laser (514.5 nm). Room temperature infrared reflectivity

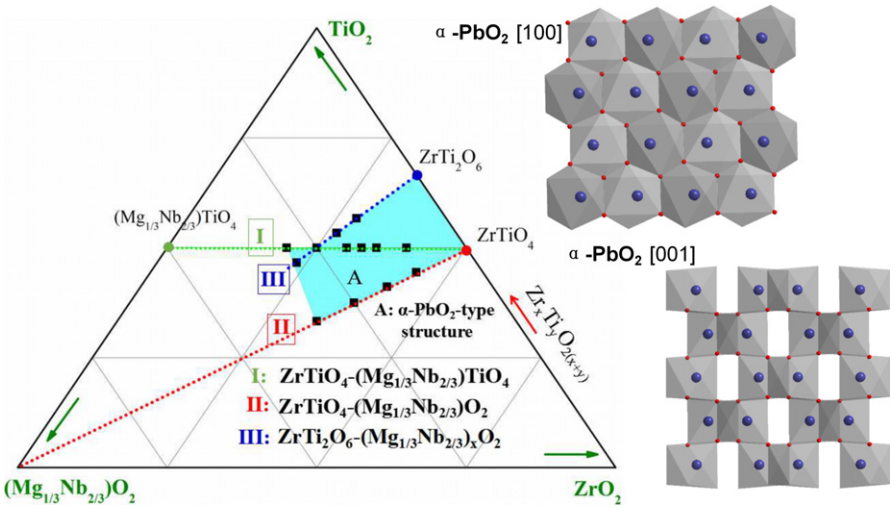

FIGURE 1 Ternary phase diagram for the system $(Mg_{1/3}Nb_{2/3})O_2$–ZrO_2–TiO_2. The $ZrTiO_4$–$(Mg_{1/3}Nb_{2/3})TiO_4$ and $(ZrTi)_{1-y}(Mg_{1/3}Nb_{2/3})_yO_4$ phases region are indicated by the black line and red line, respectively. The α-PbO_2 phase of region A is indicated by the cyan areas [Color figure can be viewed at wileyonlinelibrary.com]

spectra were measured, using a Bruker IFS 66v FT-IR spectrometer on the infrared beamline station (U4) at the National Synchrotron Radiation Lab (NSRL), China. Microwave dielectric behaviors were measured with the $TE_{01\delta}$ shielded cavity method with a network analyzer (8720ES, Agilent, Palo Alto, CA) and a temperature chamber (Delta 9023, Delta Design, Powa CA) in the temperature range of 25°C-85°C. Temperature coefficient of resonant frequency (TCF or τ_f value) was calculated with the following formula:

$$\tau_f = \frac{f_{85} - f_{25}}{f_{25}(85-25)} \times 10^6 \text{ppm/°C}, \quad (1)$$

where f_{85} and f_{25} were the $TE_{01\delta}$ resonant frequencies at 85°C and 25°C, respectively.

3 | RESULTS AND DISCUSSIONS

Figure 2 shows XRD patterns of the $(1-x)ZrTiO_4-x(Mg_{1/3}Nb_{2/3})TiO_4$ ($0.325\le x\le 0.4$) and $(ZrTi)_{1-y}(Mg_{1/3}Nb_{2/3})_yO_4$ ($0.2\le y\le 0.5$) ceramics sintered at optimal temperatures for 2 hours with 0.5 wt % $MnCO_3$ addition. The peaks are indexed, using the standard PDF cards of $ZrTiO_4$ (PDF code: 34-0415). It is found that all the diffraction peaks of the $(1-x)ZrTiO_4-x(Mg_{1/3}Nb_{2/3})TiO_4$ ($0.325\le x\le 0.4$) and $(ZrTi)_{1-y}(Mg_{1/3}Nb_{2/3})_yO_4$ ($0.2\le y\le 0.5$) ceramic sintered at 1240°C could be indexed as α-PbO_2-type structure [space group *Pnab* (60)], which is shown in Figure 1. However, some tiny peaks corresponding to the $(Mg_{1/3}Nb_{2/3})TiO_4$ phase in Figure 2A. The Pb-site cation is coordinated by 6 oxygen ions forming PbO_6 octahedra. Based on the Shannon's data, equivalent ionic radii of Zr^{4+} ions with coordination numbers (CN=6) is 0.72 Å. The equivalent ionic radii of $(Mg_{1/3}Nb_{2/3})^{4+}$ ions can be calculated by the following equation: $r=1/3R(Mg^{2+})+2/3R(Nb^{5+})=0.67$ Å (ionic radii for Mg^{2+} and Nb^{5+} are 0.72 Å and 0.64 Å, respectively).[27] The result shows that the equivalent ionic radii of $(Mg_{1/3}Nb_{2/3})^{4+}$ is smaller than that of Zr^{4+} (0.72 Å), it is understandable that the $(Mg_{1/3}Nb_{2/3})^{4+}$ ion can occupy the Zr^{4+} sites. Moreover, the $(Mg_{1/3}Nb_{2/3})^{4+}$ is larger than that of Ti^{4+} (0.604 Å). It is believed that $(Mg_{1/3}Nb_{2/3})^{4+}$ ions are more likely to enter Zr^{4+} site in the $(1-x)ZrTiO_4-x(Mg_{1/3}Nb_{2/3})TiO_4$ ($0.325\le x\le 0.4$) and $(ZrTi)_{1-y}(Mg_{1/3}Nb_{2/3})_yO_4$ ($0.2\le y\le 0.5$) ceramics. The XRD results indicates that α-PbO_2-type solid solution was formed in the 0.5 wt% $MnCO_3$-doped $(1-x)ZrTiO_4-x(Mg_{1/3}Nb_{2/3})TiO_4$ ($0.325\le x\le 0.4$) and $(ZrTi)_{1-y}(Mg_{1/3}Nb_{2/3})_yO_4$ ($0.2\le y\le 0.5$) ceramics.

SEM images of cross-section of the 0.5 wt% $MnCO_3$-doped $(1-x)ZrTiO_4-x(Mg_{1/3}Nb_{2/3})TiO_4$ (x=0.325, 0.35, 0.4) and $(ZrTi)_{(1-y)}(Mg_{1/3}Nb_{2/3})_yO_4$ (y=0.2, 0.3, 0.4) ceramics sintered at optimal temperatures for 2 hours are depicted in Figure 3. From Figure 3A-C, it can be seen that dense microstructures were observed and the average grain size of the $ZrTiO_4-(Mg_{1/3}Nb_{2/3})TiO_4-0.5$ wt% $MnCO_3$ ceramic is in the range of 4-5 μm. The $(ZrTi)(Mg_{1/3}Nb_{2/3})TiO_4-0.5$ wt% $MnCO_3$ ceramics have less porous microstructures in Figure 3C,D. Compared with the $ZrTiO_4-(Mg_{1/3}Nb_{2/3})TiO_4-0.5$ wt% $MnCO_3$ ceramic, the average grain sizes of $(ZrTi)(Mg_{1/3}Nb_{2/3})TiO_4-0.5$ wt% $MnCO_3$ ceramics are much larger.

Figure 4 shows the density and microwave dielectric properties of the $(1-x)ZrTiO_4-x(Mg_{1/3}Nb_{2/3})TiO_4$ ($0.325\le x\le 0.4$) ceramics with 0.5 wt% $MnCO_3$ sintered at temperatures ranging from 1200°C to 1260°C as a function of $(Mg_{1/3}Nb_{2/3})TiO_4$ addition. From Figure 4A, the density of sample increases with the increase of $(Mg_{1/3}Nb_{2/3})TiO_4$. It should be related to the solubilization of $(Mg_{1/3}Nb_{2/3})^{4+}$ ions into the sites of Zr^{4+} ions. The densities of the sample sintered at

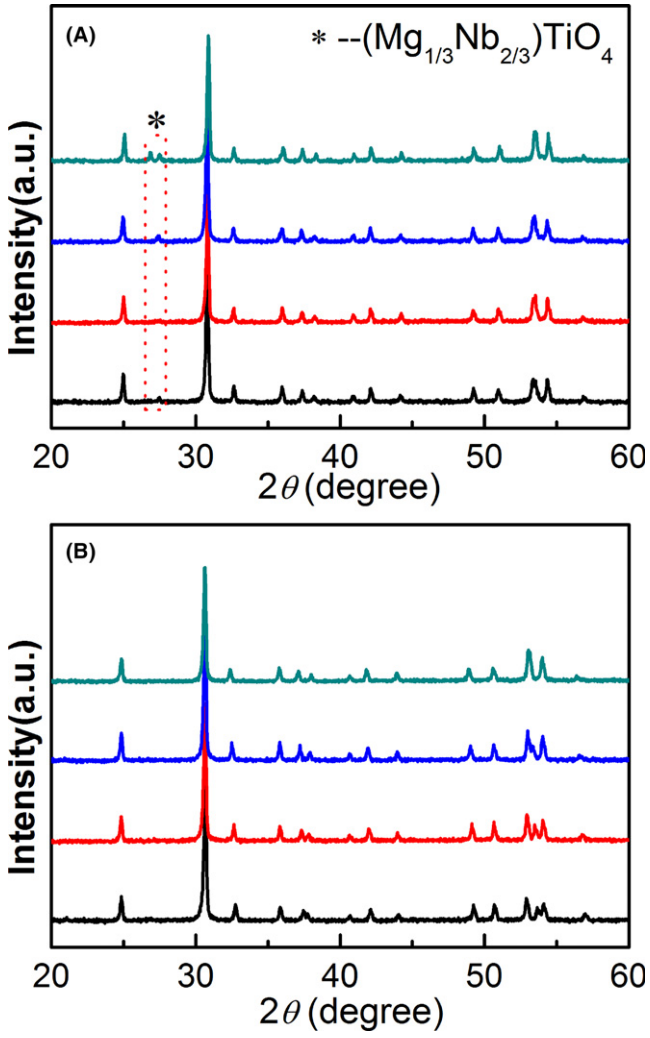

FIGURE 2 XRD patterns of the sintered 0.5 wt% $MnCO_3$-doped $(1-x)ZrTiO_4-x(Mg_{1/3}Nb_{2/3})TiO_4$ (A) and $(ZrTi)_{1-y}(Mg_{1/3}Nb_{2/3})_yO_4$ (B) ceramics [Color figure can be viewed at wileyonlinelibrary.com]

1240°C for 2 hours show the maximum apparent density 4.85 g/cm^3 at x=0.375. Permittivity of the sample increased firstly with the $(Mg_{1/3}Nb_{2/3})TiO_4$ addition from x=0.325 to 0.375, and then decreased at x=0.4. Permittivity of samples sintered at 1240°C increased first from 42.6 to maximum value of 44.2, and then reduced to 43.5. Figure 4C,D shows $Q\times f$ and τ_f values of the $(1-x)ZrTiO_4-x(Mg_{1/3}Nb_{2/3})TiO_4$ ($0.325\le x\le 0.4$) ceramics with 0.5 wt% $MnCO_3$ addition sintered at temperatures ranging from 1200°C to 1260°C as a function of the $(Mg_{1/3}Nb_{2/3})TiO_4$ addition. The variation in $Q\times f$ value versus sintering temperature presented similar behavior to that of permittivity, the $Q\times f$ values increased and then decreased rapidly as the $(Mg_{1/3}Nb_{2/3})TiO_4$ addition was increased further. As shown in Figure 4D, the τ_f value increased gradually step by step with x value. High performance of microwave dielectric properties of the $0.65ZrTiO_4-0.35(Mg_{1/3}Nb_{2/3})TiO_4$ ceramic can be obtained sintered at 1240°C for 2 hours with ε_r~44.2, $Q\times f$~40 030 GHz and τ_f~−10.1 ppm/°C. Table 1 shows the microwave dielectric properties of the $(ZrTi)_{1-y}(Mg_{1/3}Nb_{2/3})_yO_4$ ($0.2\le y\le 0.5$) ceramics with 0.5 wt% $MnCO_3$ sintered at optimized sintering temperature. The samples can be sintered well at 1200°C~1260°C with ε_r of 31.5-33.2, the $Q\times f$ values of 24 100-38 600 GHz, and the τ_f values of −23 ppm/°C to 6 ppm/°C. The $(ZrTi)_{1-y}(Mg_{1/3}Nb_{2/3})_yO_4$ ceramics can be obtained the best microwave dielectric properties with permittivity ~31.8,$Q\times f$~35 640 GHz and τ_f~−5.9 ppm/°C when y=0.3.

Raman spectroscopy is a useful tool to study the structures and identify vibrational modes of solid materials.[28-30] Figure 5 shows room-temperature Raman spectrum of the 0.5 wt% $MnCO_3$-doped $0.65ZrTiO_4-0.35(Mg_{1/3}Nb_{2/3})TiO_4$ and $(ZrTi)_{0.7}(Mg_{1/3}Nb_{2/3})_{0.3}O_4$ ceramics over the range 150-900 cm^{-1}. $ZrTiO_4$ with a random distribution of zirconium and titanium ions (taking zirconium and titanium ions as one type of averaged ion) has an orthorhombic α-PbO_2 structure (space group *Pbcn*). Using the factor group analysis, the phonons of $ZrTiO_4$ in the Γ-point of the first Brillouin zone can be described as follows:[31]

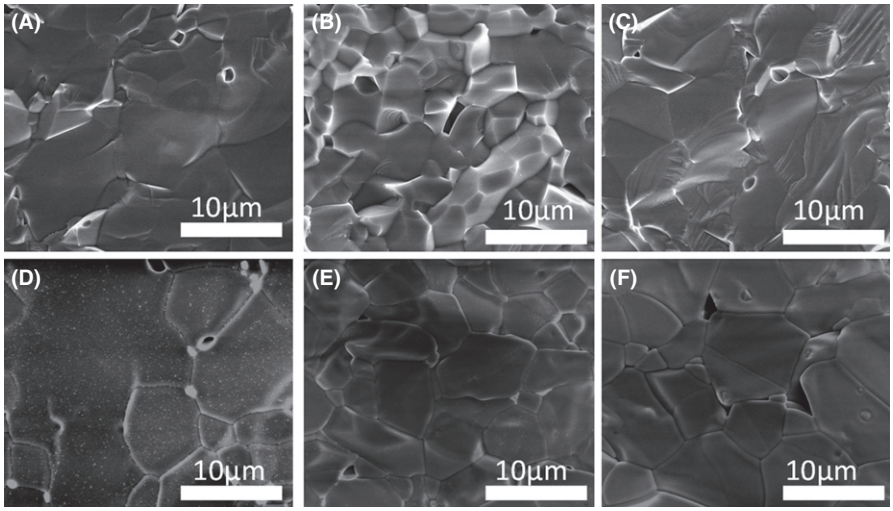

FIGURE 3 SEM images of fractured surface of the sintered 0.5 wt% $MnCO_3$-doped $(1-x)ZrTiO_4-x(Mg_{1/3}Nb_{2/3})TiO_4$: x=0.325 (A), x=0.35 (B), x=0.375 (C) and $(ZrTi)_{1-x}(Mg_{1/3}Nb_{2/3})_xO_4$: y=0.2 (D), y=0.3 (E), y=0.4 (F) ceramics

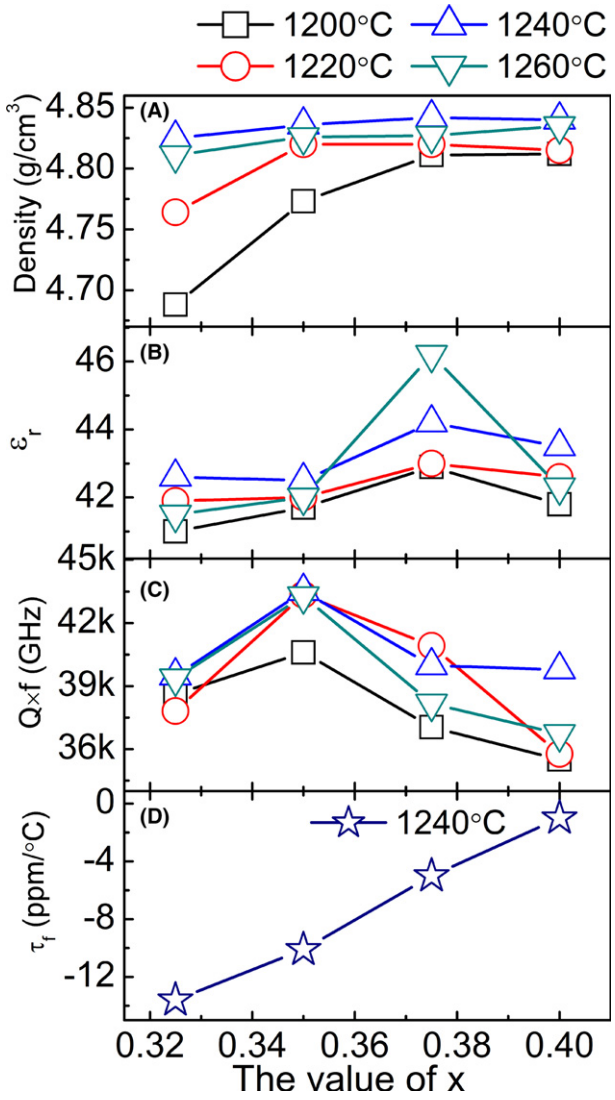

FIGURE 4 The density and microwave dielectric properties of 0.5 wt% $MnCO_3$-doped $(1-x)ZrTiO_4-x(Mg_{1/3}Nb_{2/3})TiO_4$ $(0.325\leq x\leq 0.4)$ ceramics as a function of x value and sintering temperature [Color figure can be viewed at wileyonlinelibrary.com]

$$\Gamma = 4A_g + 5B_{1g} + 4B_{2g} + 5B_{3g} + 4A_u + 3B_{2u} + 4B_{3u} \quad (2)$$

According to the literature, 18 Raman active ($4A_g$+$5B_{1g}$+$4B_{2g}$+$5B_{3g}$) and 11 infrared active ($4A_u$+$4B_{1u}$+$3B_{2u}$) modes are predicted.[32]

As shown in Figure 5, it is indicated that the substitution of Zr^{4+} by $(Mg_{1/3}Nb_{2/3})^{4+}$ influenced the number, intensity and location of the Raman bands. When Zr^{4+} ions is replaced by the $(Mg_{1/3}Nb_{2/3})^{4+}$ ions, less Raman bands appear and most of the peaks become broader. Some weak Raman bands of $ZrTiO_4$, such as those centered at 397 cm^{-1}, and 730 cm^{-1} disappeared with the substitution of Zr^{4+} by $(Mg_{1/3}Nb_{2/3})^{4+}$ in Figure 5. The number of visible Raman bands of 0.5 wt% $MnCO_3$-doped $0.65ZrTiO_4-0.35(Mg_{1/3}Nb_{2/3})TiO_4$ and $(ZrTi)_{0.7}(Mg_{1/3}Nb_{2/3})_{0.3}O_4$ ceramics are 11 and 10 in the range of 150 cm^{-1} to 900 cm^{-1}, respectively. In order to observe the lattice vibrational modes, the peaks were fitted by the standard Gaussia-Lorentzian model, and the fitted Raman spectra are plotted in Figure 5 as solid lines. In this study, the expected wavenumbers of the characteristic bands of TiO_4 tetrahedron are 306 cm^{-1}, 371 cm^{-1}, 761 cm^{-1}, 770 cm^{-1} and that of ZrO_4 tetrahedron are 332 cm^{-1}, 387 cm^{-1}, 792 cm^{-1}, and 846 cm^{-1}. Three bands centered at 271 cm^{-1}, 406 cm^{-1}, 640 cm^{-1} are assigned to vibrational modes $Ti(Zr)O_6$ octahedron.[33] Since $(Mg_{1/3}Nb_{2/3})^{4+}$ ions are more likely to enter Zr^{4+} site substituting Zr^{4+}, a (MgNb)−O bond is formed and the length of the (MgNb)−O bond is shorter than that of the Zr−O bond in the lattice. Based on Raman data in Figure 5, the spectrum recorded in the studied system is in good agreement with that of the previously reported $Zr_{1-x}(Li_{1/4}Nb_{3/4})_xTiO_4$ $(0\leq x\leq 0.5)$ samples.[25,26]

Figure 6 presents IR reflectivity spectra of the $0.65ZrTiO_4$–$0.35(Mg_{1/3}Nb_{2/3})TiO_4$ and $(ZrTi)_{0.7}(Mg_{1/3}$

TABLE 1 Microwave dielectric properties of 0.5 wt% $MnCO_3$-doped temperature stable ceramics $(Mg_{1/3}Nb_{2/3})O_2$–ZrO_2–TiO_2 ternary system

No.	Composition	S.T. (°C)	ε_r	$Q\times f$ (GHz)	τ_f(ppm/°C)
1	$(Mg_{1/3}Nb_{2/3})TiO_4$	1220	81.9	13 380	+277.5
2	$0.675ZrTiO_4$–$0.325(Mg_{1/3}Nb_{2/3})TiO_4$	1240	42.6	39 490	−13.6
3	$0.65ZrTiO_4$–$0.35(Mg_{1/3}Nb_{2/3})TiO_4$	1240	42.5	43 510	−10.1
4	$0.625ZrTiO_4$–$0.375(Mg_{1/3}Nb_{2/3})TiO_4$	1260	44.2	39 980	−5
5	$0.6ZrTiO_4$–$0.4(Mg_{1/3}Nb_{2/3})TiO_4$	1240	43.5	39 780	−1
6	$(ZrTi)_{0.8}(Mg_{1/3}Nb_{2/3})_{0.2}O_4$	1260	33.0	24 100	+6
7	$(ZrTi)_{0.7}(Mg_{1/3}Nb_{2/3})_{0.3}O_4$	1260	31.8	35 640	−5.9
8	$(ZrTi)_{0.6}(Mg_{1/3}Nb_{2/3})_{0.4}O_4$	1260	31.5	28 000	−12
9	$(ZrTi)_{0.5}(Mg_{1/3}Nb_{2/3})_{0.5}O_4$	1220	33.2	38 600	−23

S.T., Sintering Temperature.

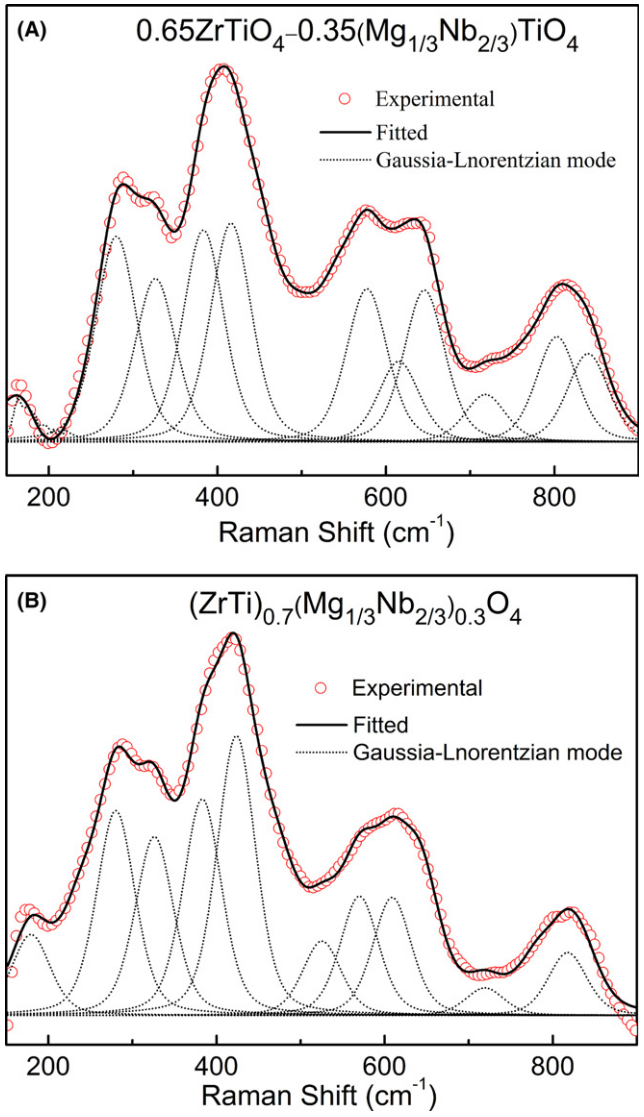

FIGURE 5 Room-temperature Raman spectra of 0.5 wt% $MnCO_3$-doped $0.65ZrTiO_4$–$0.35(Mg_{1/3}Nb_{2/3})TiO_4$ (A) and $(ZrTi)_{0.7}(Mg_{1/3}Nb_{2/3})_{0.3}O_4$ (B) ceramics sintered at 1240°C. (Circles show the observed data, thick black solid line give the model fit and the dashed line indicates the Gaussian-Lorentzian mode fitting) [Color figure can be viewed at wileyonlinelibrary.com]

$Nb_{2/3})_{0.3}O_4$ ceramics with 0.5 wt% $MnCO_3$ addition in the range 100 cm^{-1}~1000 cm^{-1}. It is seen that the infrared spectra can be well fitted by 8 resonant modes which is less than the predicted value by group theory analysis mentioned above. The measured spectrum was similar to that of the $ZrTiO_4$. These spectra were analyzed, using the classical harmonic oscillator model based on the standard Lorentzian formula [Equation (3)] and the Fresnel formula [Equation (4)]:[34,35]

$$\varepsilon^*(\omega) = \varepsilon_\infty + \sum_{j=1}^{n} \frac{\omega_{pj}^2}{\omega_{oj}^2 - \omega^2 - i\gamma_j\omega} \tag{3}$$

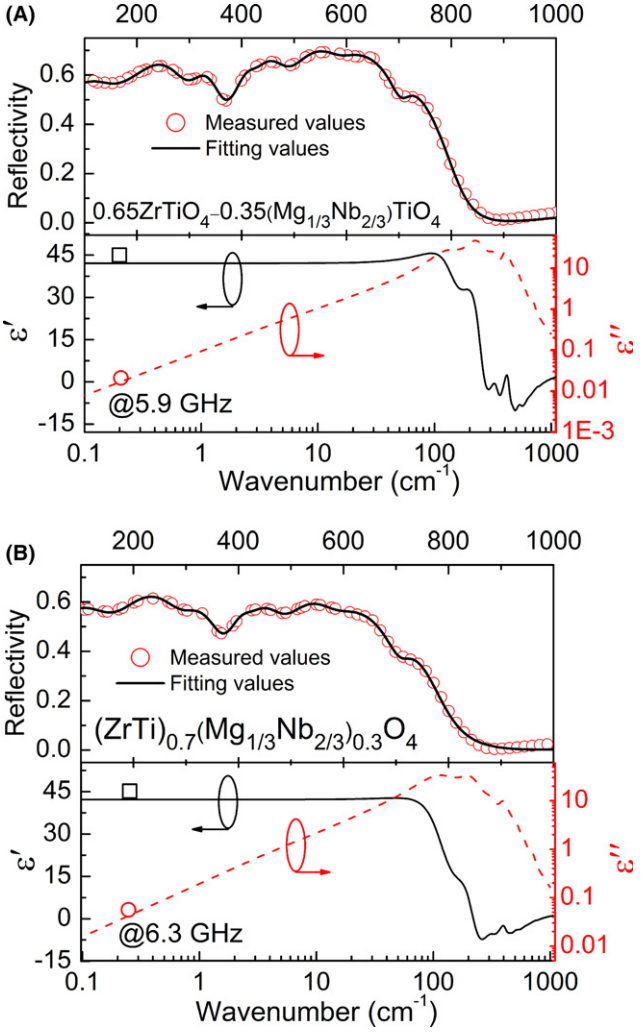

FIGURE 6 Measured and calculated infrared reflectivity spectra and complex dielectric spectra of 0.5 wt% $MnCO_3$-doped $0.65ZrTiO_4$–$0.35(Mg_{1/3}Nb_{2/3})TiO_4$ (A) and $(ZrTi)_{0.7}(Mg_{1/3}Nb_{2/3})_{0.3}O_4$ (B) ceramic (solid line for fitting values and hollow symbol for measured values, circles are experimental at microwave region, and solid lines represent the fit of IR spectra) [Color figure can be viewed at wileyonlinelibrary.com]

$$R(\omega) = \left| \frac{1 - \sqrt{\varepsilon^*(\omega)}}{1 + \sqrt{\varepsilon^*(\omega)}} \right|^2, \tag{4}$$

where $\varepsilon^*(\omega)$ is complex dielectric function; ε_∞ is the dielectric constant caused by the electronic polarization at high frequencies; ω_{pj}, ω_{oj}, and γ_j are the plasma frequency, the transverse frequency, and damping factor of the *j*-th Lorentz oscillator, respectively; *n* is the number of transverse phonon modes; $R(\omega)$ is the IR reflectivity.

Figure 6 is also shown the calculated permittivity $\varepsilon'(\omega)$ and loss $\varepsilon''(\omega)$ obtained from the fits of the infrared reflectivity together with the experimental microwave data. The fitting of the infrared reflectivity spectra of the 0.5 wt% $MnCO_3$-doped $0.65ZrTiO_4$–$0.35(Mg_{1/3}Nb_{2/3})$

TiO_4 and $(ZrTi)_{0.7}(Mg_{1/3}Nb_{2/3})_{0.3}O_4$ ceramics. It is observed that the calculated ε_r is a little smaller than the measured ones in the microwave range. Meanwhile, all the calculated dielectric permittivity and dielectric loss values are nearly equal to the measured ones, using $TE_{01\delta}$ method. Therefore, it can be concluded that majority of the dielectric contribution for $(Mg_{1/3}Nb_{2/3})O_2$–ZrO_2–TiO_2 system at the microwave region was attributed to the absorptions of phonon oscillation at infrared region and very little contribution from defect phonon scattering.

4 | CONCLUSION

In the present work, the 0.5 wt% $MnCO_3$-doped $(1-x)ZrTiO_4-x(Mg_{1/3}Nb_{2/3})TiO_4$ $(0.325\leq x\leq 0.4)$ and $(ZrTi)_{1-y}(Mg_{1/3}Nb_{2/3})_yO_4$ $(0.2\leq y\leq 0.5)$ ceramics were obtained at low sintering temperatures. High performance of microwave dielectric properties can be obtained in the $0.65ZrTiO_4-0.35(Mg_{1/3}Nb_{2/3})TiO_4$ ceramics with ε_r of 42.5, $Q\times f$ values of 43 520 GHz (at 5.9 GHz), and near zero τ_f values of −5 ppm/°C. Meanwhile, the $(ZrTi)_{0.7}(Mg_{1/3}Nb_{2/3})_{0.3}O_4$ ceramic sintered at 1260°C for 2 hours with a ε_r of 31.8, a $Q\times f$ value of 35 640 GHz and a near zero τ_f value of −5.9 ppm/°C. The Raman spectrum and infrared spectra analysis indicated that the majority of the dielectric polarization at microwave frequency was contributed by the phonon oscillation.

ACKNOWLEDGMENTS

This work was supported by the National Natural Science Foundation of China (U1632146), the Young Star Project of Science and Technology of Shaanxi Province (2016KJXX-34, 2015KJXX-39), the Fundamental Research Funds for the Central University, and the 111 Project of China (B14040). The authors thank the administrators in IR beamline workstation of National Synchrotron Radiation Laboratory (NSRL) for their help in the IR measurement. SEM work was performed at the International Center for Dielectric Research (ICDR), Xi'an Jiaotong University, Xi'an, China.

REFERENCES

1. Reaney IM, Iddles D. Microwave dielectric ceramics for resonators and filters in mobile phone networks. *J Am Ceram Soc*. 2006;89:2063-2072.
2. Rodriguez MA, Yang P, Kotula P, Dimos D. Microstructure and phase development of buried resistors in low temperature co-fired ceramic. *J Electroceram*. 2000;5:217-223.
3. Sebastian MT, Jantunen H. Low loss dielectric materials for LTCC applications: a review. *Int Mater Rev*. 2008;53:57-90.
4. Subodh G, Sebastian MT. Glass-free $Zn_2Te_3O_8$ microwave ceramic for LTCC. *J Am Ceram Soc*. 2007;90:2266-2268.
5. Valant M, Suvorov D. Chemical compatibility between silver electrodes and low-firing binary-oxide compounds: conceptual study. *J Am Ceram Soc*. 2000;83:2721-2729.
6. Pang LX, Zhou D, Qi ZM, Liu WG, Yue ZX, Reaney IM. Structure-property relationships of low sintering temperature scheelite-structured (1-x)$BiVO_4$–x$LaNbO_4$ microwave dielectric ceramics. *J Mater Chem C*. 2017;5:2695-2701.
7. Templeton A, Wang XR, Penn SJ, Webb SJ, Cohen LF, Alford NM. Microwave dielectric loss of titanium oxide. *J Am Ceram Soc*. 2000;83:95-100.
8. Li WB, Zhou D, Xi HH, Pang LX, Yao X. Structure, infrared reflectivity and microwave dielectric properties of $(Na_{0.5}La_{0.5})MoO_4$–$(Na_{0.5}Bi_{0.5})MoO_4$ ceramics. *J Am Ceram Soc*. 2016;99:2083-2088.
9. Zhou D, Pang LX, Guo J, et al. Influence of Ce substitution for Bi in $BiVO_4$ and the impact on the phase evolution and microwave dielectric properties. *Inorg Chem*. 2014;53:1048-1055.
10. Zhou D, Guo D, Li WB, et al. Novel temperature stable high-ε_r microwave dielectrics in the Bi_2O_3-TiO_2-V_2O_5 system. *J Mater Chem C*. 2016;4:5357-5362.
11. Choi GK, Kim JR, Yoon SH, Hong KS. Microwave dielectric properties of scheelite (A=Ca, Sr, Ba) and wolframite (A=Mg, Zn, Mn) $AMoO_4$ compounds. *J Eur Ceram Soc*. 2007;27:3063-3067.
12. Zhou D, Li WB, Xi HH, Pang LX, Pang GS. Phase composition, crystal structure, infrared reflectivity and microwave dielectric properties of temperature stable composite ceramics (scheelite and zircon-type) in $BiVO_4$–YVO_4 system. *J Mater Chem C*. 2015;3:2582-2588.
13. Kim YK, Jang HM. Lattice contraction and cation ordering of $ZrTiO_4$ in the normal-to-incommensurate phase transition. *J Appl Phys*. 2001;89:6349-6355.
14. Kim YK, Jang HM. Polarization leakage and asymmetric Raman line broadening in microwave dielectric $ZrTiO_4$. *J Phys Chem Solids*. 2003;64:1271-1278.
15. Ličina V, Gajović A, Moguš-Milanković A. Correlation between the microstructure and the electrical properties of $ZrTiO_4$ ceramics. *J Am Ceram Soc*. 2008;91:178-186.
16. Wolfram G, Göbel HE. Existence range, structural and dielectric properties of $Zr_xTi_ySn_zO_4$ ceramics (x+y+z=2). *Mater Res Bull*. 1981;16:1455-1463.
17. Wang JS, Yu YL, Li S, Guo LM, Wang EJ, Cao YA. Doping behavior of Zr^{4+} ions in Zr^{4+}-doped TiO_2 nanoparticles. *J Phys Chem C*. 2013;117:27120-27126.
18. Kim KS, Kim S, Kim YH, Yoon SO, Park JG. Sintering behavior and microwave dielectric properties of the $Zr_{1-x}(Zn_{1/3}Nb_{2/3})_xTiO_4$ system with zinc-borosilicate glass. *J Ceram Process Res*. 2008;9:126-130.
19. Kim WS, Kim JK, Kim JH, Hur KH. Influence of ZnO–Nb_2O_5 substitution on microwave dielectric properties of the $ZrTiO_4$ system. *J Korean Ceram Soc*. 2003;40:346-349.
20. Liao QW, Li LX, Ding X. Phase constitution, structure analysis and microwave dielectric properties of $Zn_{0.5}Ti_{1-x}Zr_xNbO_4$ ceramics. *Solid State Sci*. 2012;14:1385-1391.
21. Tang B, Yu SQ, Chen HT, Zhang SR, Zhou XH. Phase structure and microwave dielectric properties of $Zr(Zn_{1/3}Nb_{2/3})_xTi_{2-x}O_6$ $(0.2 \leq x \leq 0.8)$ ceramics. *J Mater Sci: Mater Electron*. 2013;24:1475-1479.

22. RiaziKhoei P, Azough F, Freer R. The influence of $ZnNb_2O_6$ on the microwave dielectric properties of $ZrTi_2O_6$ ceramics. *J Am Ceram Soc*. 2006;89:216-223.
23. Kim WS, Kim JH, Kim JH, Hur KH, Lee JY. Microwave dielectric properties of the ZrO_2–ZnO–Ta_2O_5–TiO_2 systems. *Mater Chem Phys*. 2003;79:204-207.
24. Huang CL, Chien YH. Low-firable high-K dielectric in the $Zr_x(Zn_{1/3}Nb_{2/3})_{1-x}TiO_4$ ceramic system. *J Alloys Compd*. 2011;509:L239-L295.
25. Pang LX, Wang H, Zhou D, Yao X. Raman spectroscopy and microwave dielectric properties of $Zr_{1-x}(Li_{1/4}Nb_{3/4})_xTiO_4$ ceramics. *Jpn J Appl Phys*. 2009;48:051403.
26. Pang LX, Wang H, Zhou D, Chen YH, Yao X. Phase evolution, Raman spectroscopy and microwave dielectric behavior of $(Li_{1/4}Nb_{3/4})$ doped ZrO_2-TiO_2 system. *Appl Phys A*. 2010;100:1205-1209.
27. Shannon R. Dielectric polarizabilities of ions in oxides and fluorides. *J Appl Phys*. 1993;73:348-366.
28. George A, Solomon S, Thomas JK, John A. Characterizations and electrical properties of $ZrTiO_4$ ceramic. *Mater Res Bull*. 2012;47:3141-3147.
29. Kim YK, Jang HM. Dawson Raman line-shape analysis of nanostructural evolution in cation-ordered $ZrTiO_4$-based dielectrics. *Solid State Commun*. 2003;127:433-437.
30. Azough F, Freer R. A Raman spectral characterization of ceramics in the system ZrO_2-TiO_2. *J Mater Sci*. 1993;28:2273-2276.
31. Gajović A, Djerdj I, Furić K, Schlögl R, Su DS. Preparation of nanostructured $ZrTiO_4$ by solid state reaction in equimolar mixture of TiO_2 and ZrO_2. *Cryst Res Technol*. 2006;41:1076-1081.
32. Dawson P, Hargreave MM, Wilkinson GR. The vibrational spectrum of zircon ($ZrSiO_4$). *J Phys C: Solid State Phys*. 1971;4:240-256.
33. Santos CC, Silva EN, Ayala AP, et al. Raman investigations of rare earth orthovanadates. *J Appl Phys*. 2007;101:053511.
34. Chen Z, Jia H, Sharafudeen K, et al. Up-conversion luminescence from single vanadate through blackbody radiation harvesting broadband near-infrared photons for photovoltaic cells. *J Alloy Compd*. 2016;663:204-210.
35. Guo J, Zhou D, Wang L, et al. Infrared spectra, Raman spectra, microwave dielectric properties and simulation for effective permittivity of temperature stable ceramics $AMoO_4$–TiO_2 (A = Ca, Sr). *Dalton Trans*. 2013;42:1483-1491.

How to cite this article: Li W-B, Zhou D, Pang L-X, et al. High quality factor microwave dielectric ceramics in the $(Mg_{1/3}Nb_{2/3})O_2$–ZrO_2–TiO_2 ternary system. *J Am Ceram Soc*. 2017;100:3982–3989. https://doi.org/10.1111/jace.14929